Continuous-time random walk of a rigid triangle

1995 J. Phys. A: Math. Gen. 28 6645

(http://iopscience.iop.org/0305-4470/28/23/016)

J. Phys. A: Math. Gen. 28 (1995) 6645–6653. Printed in the UK

Continuous-time random walk of a rigid triangle

I M Sokolov†, R Vogel, P A Alemany‡ and A Blumen

Theoretische Polymerphysik, Universität Freiburg, Rheinstraße 12, D-79104 Freiburg i. Br., Germany

Received 15 June 1995

Abstract. We study as an example of a continuous-time random walk (CTRW) scheme under holonomic contraints the motion of a rigid triangle, moving on a plane by flips of its vertices. This interpolates between our former model of a dumbbell (two walkers joined by a fixed segment) and the Orwoll–Stockmeyer model for polymer diffusion. The jumps of the vertices follow either Poissonian or power-law waiting-time distributions, and each vertex follows its own internal clock. Numerical simulations of the triangle's centre-of-mass motion show it to be diffusive at short and also at long times, with a broad crossover (subdiffusive) region in between. Furthermore, we provide approximate expressions for the long-time regime and generalize our findings for systems of N random walkers.

1. Introduction

Many physical situations correspond to a set of random walkers which move under constraints. A typical example is a polymer. Thus the Orwoll–Stockmeyer model [1,2] pictures a macromolecular chain as a set of beads (walkers), connected to each other by rigid bonds. The chain moves by flips of the beads. In a previous work [3] we have considered the special case of a dumbbell, i.e. a rod-like molecule whose ends perform random motions, constrained by the fixed length of the rod. One may also envisage a more complicated situation, such as an oligomer in a viscous solution. In all these cases the rigidity of the bonds represents holonomic constraints. In the theory of glasses one encounters tunnel processes, which involve correlated motions of large clusters of atoms; here is again a situation whose constraints may be viewed as holonomic, although the geometrical factors involved may correspond to rather complex functional forms.

Now the random walkers may perform their jumps according to a fixed (discrete) frequency or, in the continuum, according to a simple exponential waiting-time density (WTD); this corresponds to a Poisson process. In general, for Poisson processes the spatial and the temporal aspects of the problem decouple. A much more interesting (and physically relevant) situation takes place when the jumps of the walkers follow more complex WTDs. A physical background is found in dense solutions or in melts, when a walker can move only when it has enough free volume at its disposal. This leads to the Glarum model [4] and to continuous-time random walks (CTRW) [5–11]. If the free volume is the result of a vacancy moving randomly, then the corresponding WTD follows a power-law. In some cases, even for WTD with long-time tails the spatial and temporal aspects of these processes

† Also at P N Lebedev Physical Institute of the Academy of Sciences of Russia, Leninski Prospekt 53, Moscow 117924, Russia.

‡ Also at Centro Atómico Bariloche (CNEA) and Instituto Balseiro (UNC), 8400 Bariloche, Argentina.

0305-4470/95/236645+09$19.50

may still decouple, which then allows the situation to be depicted in an elegant way, see [7, 8] for discussions. In the case that the random walkers are coupled through geometric correlations introduced by constraints (say for Orwoll–Stockmeyer polymers [12] or for dumbbells performing walks by flipping along a line [3]) the memory effects inherent in the power-law WTDs show up, and the overall behaviour is much richer. We also mention that models of coupled continuous time processes may be of interest in many areas, such as, say, in the theory of random noises, when describing the response of some appliance to correlated sequences of pulses arriving at its different entrances.

In our previous work [3] we considered the motion of a rigid dumbbell (consisting of two beads connected by a segment), which diffuses along a line by performing flips. The flips are caused by the jumps of the beads; the jumping times of each bead are independent of the others and follow a given WTD. We have shown that under geometrical constraints and broad WTD the spatial and temporal aspects of the dumbbell's motion are strongly coupled. Thus the overall motion of the dumbbell's centre of mass (CM) resembles that of a ploymer, in that two very distinct diffusion regimes at very short and at long times are separated by a wide crossover region of subdiffusive motion in between.

Now, the one-dimensional character of the dumbbell's motion simplifies the problem considerably and also leads to some features that do not persist in higher dimensions. Moreover, the presence of only two walkers (the two ends of the dumbbell) renders the problem somewhat degenerate, in the sense that it does not allow to distinguish between jump clusterization and pinning effects (vide infra). Therefore it is interesting to consider the generalization of this type of motion for higher dimensions and for a larger number of walkers involved. In this article we focus mainly on the motion in two dimensions, by considering the diffusion of a rigid equilateral triangle of sidelength c, whose vertices move. When one vertex jumps, the triangle flips around the side whose two vertices are at rest. Each vertex jumps independently of the other ones, always following its own internal clock (WTD). In the following we investigate first the motion of the triangle's CM via numerical simulations and then provide analytical approximations for the long-time diffusion coefficients. In the case of power-law WTD, the numerical simulations show that the triangle's centre of mass moves diffusively at short and also at long times, with a broad cross-over region in between. The reason for this is pinning: there is no overall translation unless all three vertices jump. We close by discussing similarities and differences between the behaviour of a triangle's random walk and that of a segment or of a chain molecule; this throws light on the statistical nature of correlated, non-Markovian stochastic processes.

2. The model

As mentioned in section 1, we analyse the motion of a rigid triangle, which moves by jumps of its vertices. A jump consists of the flip of a vertex around the opposite side, while keeping the two other vertices fixed. The triangle's CM moves at each jump over a distance $a = c/\sqrt{3}$. For simplicity we set $c = \sqrt{3}$ so that $a = 1$. The overall motion of the CM is then a random walk performed on a hexagonal lattice of unit sidelength, see figure 1.

The jumps occur in continuous time, so that we now introduce $\psi(t)$, the waiting-time density (WTD) between the jumps of the same vertex, the jumps of distinct vertices being uncorrelated. We focus on processes which are homogeneous in time, and hence correspond to equilibrium renewal processes (RP) [13]. We distinguish between WTDs of exponential type

$$\psi(t) = \lambda e^{-\lambda t} \tag{1}$$

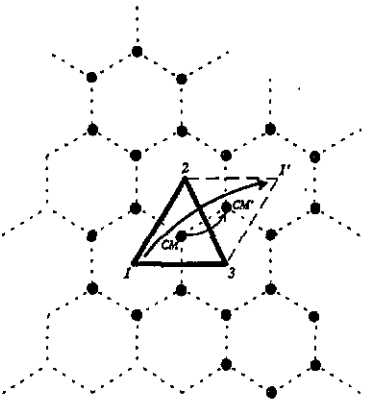

Figure 1. Displacements of the triangle starting with a jump of vertex 1. The triangle's CM performs a random walk on a two-dimensional hexgonal lattice indicated through broken curves. All sites (dots) which can be reached by the CM within one step of vertex 1 are also shown, see text for details.

which lead to Poisson processes and between WTD with long-time tails. As a suitable form for the latter we choose

$$\psi(t) = \gamma(1+t)^{-1-\gamma} \tag{2}$$

with $\gamma > 1$. The WTD (2) is well defined for all times $t \geqslant 0$ and behaves algebraically, $\psi(t) \propto \gamma/t^{\gamma+1}$, for t large.

Equilibrium RP correspond to a situation in which all vertices have started their motion long ago, before the beginning of the observations at $t = 0$. In this caes the WTD for the first jump of each vertex after $t = 0$, $\psi_1(t)$, may have a different form from the WTD for all subsequent jumps, $\psi(t)$.

Let $\langle t \rangle$ denote the mean waiting time between jumps; $\langle t \rangle$ equals $1/\lambda$ for the exponential WTD, equation (1) and $1/(\gamma - 1)$ for the long-time tailed WTD, equation (2). Furthermore, the survival probability $\phi(t)$, i.e. the probability that up to a time t after the last jump no further jump occurred, equals

$$\phi(t) = \int_t^\infty \mathrm{d}t' \psi(t'). \tag{3}$$

Now $\psi_1(t)$ coincides with the equilibrium forward waiting time density [13, 14], and in terms of $\phi(t)$ and $\langle t \rangle$ is given by:

$$\psi_1(t) = \phi(t)/\langle t \rangle. \tag{4}$$

One verifies now readily that for the exponential WTD $\psi(t)$ and $\psi_1(t)$ are identical. For WTDs of the type of equation (2) $\psi_1(t)$ is given by

$$\psi_1(t) = (\gamma - 1)(1+t)^{-\gamma} \tag{5}$$

and hence differs from $\psi(t)$.

3. Simulation results

Our numerical simulations of the triangle's motion are quite straightforward. For each realization of the motion we compute first the times between jumps for each of the three vertices. We do this for each vertex separately, by listing the times at which the vertex

jumps, such that the first jump follows the distribution $\psi_1(t)$ and the waiting times for following jumps the distribution $\psi(t)$. This leads to three separate lists. Then we order all jumps in a single list, in ascending order, and move the triangle according to this list. We store both the times and the coordinates of the triangle's CM after each jump, thus obtaining a trajectory of the triangle's motion. Some 10^5 to 10^6 such trajectories were generated for each choice of the WTD; such numbers were deemed necessary, in order to get statistically consistent results.

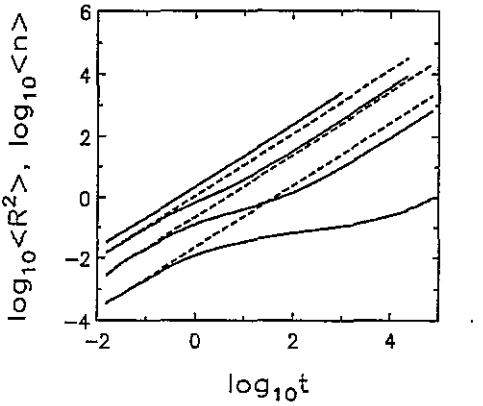

Figure 2. Mean square displacement $\langle R^2(t)\rangle$ of the triangle's CM (full curve) and $\langle n(t)\rangle$, the average number of jumps (broken curve) during time t. The results for the exponential WTD, equation (1) and for the long-time tailed algebraic WTDs, equation (2) for $\gamma = 1.5$, 1.1 and 1.01 (from top to botttom). For the exponential WTD both lines coincide, whereas $\langle R^2(t)\rangle$ and $\langle n(t)\rangle$ differ for the WTDs of equation (2).

Figure 2 shows simulation results for the mean squared displacement $\langle R^2(t)\rangle$ and for the mean overall number of jumps $\langle n(t)\rangle$ of the triangle's CM as a function of time. Both the exponential WTD, equation (1) and also WTDs with long-time tails, equation (2) are analysed for a whole series of values of the parameter γ. We note that in the units used and for the exponential WTD $\langle R^2(t)\rangle$ and $\langle n(t)\rangle$ coincide and depend linearly on t. For power-law WTDs the behaviour of $\langle R^2(t)\rangle$ and $\langle n(t)\rangle$ is different: while the mean number of jumps is still proportional to t, $\langle R^2(t)\rangle$ is not. In fact $\langle R^2(t)\rangle$ shows a diffusive behaviour at short and at long times, and a subdiffusive behaviour in between. Note that in figure 2 the scales are logarithmic and that the different dynamical regimes often stretch over several orders of magnitude in time.

In the case of exponential WTDs the related RP is a Poisson process, whose events (jumps) are uniformly distributed in time. The pooled process (i.e. the process corresponding to the superposition of all events) is also a Poisson process, albeit with a correspondingly reduced parameter λ; this process is statistically indistinguishable from the one in which first the pooled Poisson output is generated and then each event is assigned the vertex which jumps. For Poisson RP the starting points of consecutive jumps are uncorrelated; furthermore it turns out that the dynamics can be decoupled into a spatial and into a temporal part [7]. The triangle's CM performs thus a random walk on the two-dimensional hexagonal lattice and its mean squared displacement turns out to be proportional to the average number of jumps; i.e. we find

$$\langle n(t)\rangle = 3t/\langle t\rangle \tag{6}$$

at all times. In equation (6) $\langle t\rangle = 1/\lambda$ is, as before, the mean waiting time between jumps

of the same vertex. This yields for the CM's mean squared displacement:

$$\langle R^2(t)\rangle = a^2\langle n(t)\rangle = 3a^2\lambda t \tag{7}$$

where $a^2 = 1$ is the mean squared displacement of the CM per jump. The behaviour of the CM is diffusive on all time scales, which fact is clearly seen in figure 2, and is due to the lack of correlations between consecutive jumps.

For broad WTD such as equation (2), consecutive jumps are correlated. The correlations arise from the fact that such WTDs have a memory of their starting time. The behaviour of the CM's motion is then more complex, as may be seen from figure 2, which shows an intermediate, subdiffusive regime. Now the short-time regime corresponds to the first jump of a single vertex. For this first event the mean squared displacement of the CM is, as before

$$\langle R^2(t)\rangle = 3a^2 t/\langle t\rangle = 3a^2(\gamma - 1)t \tag{8}$$

i.e. a diffusive behaviour. This regime is followed quite quickly by a subdiffusive behaviour. In the long-time regime the behaviour is again diffusive, with a much smaller diffusion constant than the one in equation (8). In figure 3 we present the values of the diffusion coefficient D in the long-time regime as a function of $\gamma - 1$. Here we have extended the range of γ to values above two, such that we also studied $\gamma = 2.5, 3, 4, 6$ and 10. As may be verified from figure 3, for large γ the diffusion coefficient D is approximately proportional to $(\gamma - 1)$, while for $\gamma \to 1$ the diffusion coefficient behaves rather as $D \propto (\gamma - 1)^3$. In what follows we will explain this type of behaviour for $\gamma \to 1$, and will estimate the magnitude of D. Note that $\gamma = 1$ is marginal; for $\gamma < 1$ no long-time diffusive region exists.

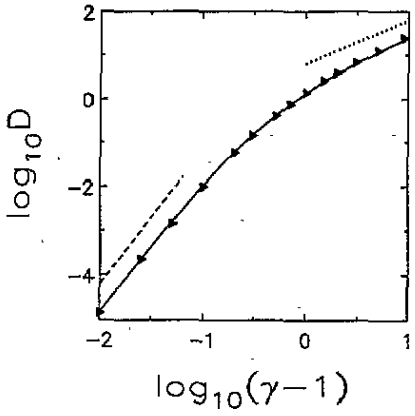

Figure 3. Long-time diffusion coefficient D as a function of $(\gamma-1)$. Note the double logarithmic scales. The full curve represents equation (13) with $k = 8$, see text for details. The broken curve has a slope of 3, the dotted curve a slope of 1; they indicate limiting behaviours.

Our approach to understanding the triangle's motion under broad WTD is based on the observation that the main effect governing the slow long-time diffusion is pinning: a large scale motion of the triangle is only possible if all its three vertices move; otherwise the triangle only rotates around its pinned vertex, a fact which leads to no translation.

4. The nature of the long-time behaviour

To clarifiy the overall character of the motion we present in figure 4 a realization of a sequence of jumps for the three vertices generated for the WTD of equation (2) with $\gamma = 1.3$.

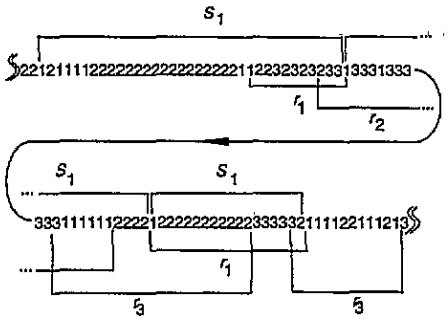

Figure 4. A sequence of jumps of three vertices, generated by the WTD, equation (2) for $\gamma = 1.3$. Here S_1 represents steps of vertex 1, r_j denotes a return of vertex j. Note the strong clusterization of jumps.

According to our numerical procedure, we have computed the independent renewal times for the three vertices, and denoted the corresponding RPs by 1, 2 and 3. Then we have arranged the jump times in ascending order and printed the sequence of the vertices which move. The first feature evident from figure 4 is the tendency of jumps of the same vertex to cluster together. Evidently, such clusters let a vertex jump back and forth, with no net diffusive effect. One may believe that this is the main reason of slowing down the diffusion. However, one can show that clusterization alone is not sufficient to explain the small values of D and the $D \propto (\gamma - 1)^3$ dependence. As mentioned above, for an overall diffusive movement of the triangle during longer time intervals it is necessary that *all* vertices jump during this time, otherwise there occur only rotations. We refer to this situation as pinning. Note that for a dumbbell (dimer) there is no difference between clusterization and pinning, while for systems built out of three or more random walkers clusterization and pinning differ, so that the pinning period of one vertex can include several clusters of jumps of the other vertices.

To take into account pinning effects we now define an (effective) step to be a shortest sequence of the events, which starts with a jump of 1 (or the beginning of such a cluster of jumps) and ends just before a jump of 1, such that in this interval both 2 and 3 have had at least one jump each. An example for a step is the sequence ...11211132231.... In figure 4 we have indicated by S_1 several steps. The end of the step (jump of 1) is the starting point of the next step. Note that steps cover the set of jumps completely, so that each jump belongs to exactly one step. We disregard further correlations by considering displacements taking place during consecutive steps to be independent of each other. One can then estimate $\langle T \rangle$, the mean duration of a step, and obtain from it an estimate for D in the form $D = b^2/\langle T \rangle$ where b^2 is the mean squared displacement of the CM per step. As we proceed to show the $D \propto (\gamma - 1)^3$ dependence stems directly from the behaviour of $\langle T \rangle$.

Our next task is then to estimate $\langle T \rangle$. Now, a step is a rather complicated sequence of jumps and it is not simple to estimate $\langle T \rangle$ straightforwardly. Nevertheless one can show that the number of steps during a given time interval can be estimated from below and from above through some other sequences of a much simpler nature, which we call returns. We denote by a return of, say vertex 1, a situation in which between two consecutive jumps of vertex 1 there occur jumps of both the two other vertices. Examples for returns are ...1231... or ...1223321.... Several returns are indicated exemplarily in figure 4. Note that returns do not cover the full set of events; e.g. the series of jumps ...121... does not

belong to any return of vertex 1.

It is evident that each return of vertex 1 corresponds to a step of the overall process: This step begins with some jump of 1 after which either this jump, or the end of a cluster of jumps of 1 which follows, is the beginning of the return considered; the step finishes with the end of the return (e.g. the first step in figure 4). On the other hand there are steps containing no returns of vertex 1 (for example, the second step in figure 4 includes no returns of 1). Therefore, the overall mean number of steps within a long time interval t is not smaller than the number of returns: $\langle n_s(t)\rangle \geqslant \langle n_r(t)\rangle$. Furthermore, one can note that the end of each step of 1 lies either within a return of 2 or within a return of 3. To show this one must notice the following: The step of 1 ends with a jump of 1 which was preceded by a jump of either 2 or 3. Let us assume for simplicity that it was 2. The structure around the end of the step 1 is then $\ldots 3xxx21xxx3\ldots$, where x denotes either 1 or 2 (or is empty). This structure shows that 1 lies now within a return of 3. This consideration shows that the overall number of steps cannot be larger than the number of returns of 2 and 3, i.e. that $\langle n_s(t)\rangle \leqslant 2\langle n_r(t)\rangle$ holds. In summary we have

$$\langle n_r(t)\rangle \leqslant \langle n_s(t)\rangle \leqslant 2\langle n_r(t)\rangle. \tag{9}$$

Let us now calculate $\langle n_r(t)\rangle$ for some vertex within a given time interval t. This number is equal to $p\langle n(t)\rangle$, with $\langle n(t)\rangle = t/\langle t\rangle$ being the mean number of jumps during t of the vertex considered, and p being the probability that an arbitrary jump of this vertex corresponds to the beginning of a return. This probability is given by

$$p = \int_0^\infty \mathrm{d}t\psi(t)[1-\phi_1(t)]^2 \tag{10}$$

where, parallelling equation (3), we have introduced $\phi_1(t) = \int_t^\infty \mathrm{d}t'\psi_1(t')$. Equation (10) means that both 2 and 3 jump before 1 jumps again. For algebraic WTDs equation (10) yields

$$p = \int_0^\infty \mathrm{d}t\gamma(1+t)^{-1-\gamma}(1-(1+t)^{1-\gamma})^2 = 2\frac{(\gamma-1)^2}{(2\gamma-1)(3\gamma-2)} \tag{11}$$

which with $\langle t\rangle = (\gamma-1)^{-1}$, see discussions after equation (2), leads to

$$\langle n_r(t)\rangle = p\frac{t}{\langle t\rangle} = \frac{2(\gamma-1)^3}{(2\gamma-1)(3\gamma-2)}t. \tag{12}$$

Together with the inequalities (9) it follows that $\langle n_s(t)\rangle$ depends linearly on t and that it goes as $(\gamma-1)^3$ for $\gamma \to 1$. Now $\langle T\rangle$ is given by $\langle T\rangle \propto t/\langle n_s(t)\rangle$ and thus $\langle T\rangle \propto (\gamma-1)^{-3}$ for $\gamma \to 1$.

To conclude that D goes as $(\gamma-1)^3$ for $\gamma \to 1$ we need an estimate for b^2, the mean squared displacement of the CM per step. Now b^2 is bounded from above: The possible positions of the triangle's CM after one step (where the step always starts with a jump of 1) are shown in figure 1. The maximal displacement per step is then $\sqrt{13}$, which gives an upper bound for b^2 of $b^2 \leqslant 13$. Evidently, the mean squared displacement achieved in a step depends on the sequence of jumps. If we now average over all positions in figure 1 as being equally possible, we arrive at $b^2 = 23/4$. This value is close to the results of the numerical simulations.

We turn now to the simulation results and approximate D for $\gamma < 2$ through

$$D = k\frac{2(\gamma-1)^3}{(2\gamma-1)(3\gamma-2)} \tag{13}$$

where the numerical factor k is taken to be a fitting parameter. For $1 < \gamma < 2$ we establish that equation (13) is an excellent choice: We find that k is statistically indistinguishable from a constant and that $k = 8.0 \pm 0.2$. In figure 3 the full curve is equation (13) with $k = 8$. In fact expression (13) works surprisingly well even for $2 < \gamma < 10$. Equation (13) can be reinterpreted in the form $D = k\langle n_r(t)\rangle/t$. This form is very adequate also for the Poisson process, for which equation (10) gives $p_r = 1/3$; with $D = 3$ this leads to $k = 9$.

Comparing the results obtained for a triangle with those of [3] for a dumbbell (i.e. for two vertices) allows us to draw some conclusions. First, in the case of a dumbbell, each step corresponds to a sequence of two clusters (one of vertex 1 and one of vertex 2) and to exactly one return of each vertex. The mean duration of a step is then proportional to $\langle T\rangle = p^{-1}\langle t\rangle = (2\gamma - 1)/(\gamma - 1)^2$, see the calculation below for an arbitrary number N of vertices. In this case D goes as $(\gamma - 1)^{-2}$ for $\gamma \to 1$, which coincides with the findings of [3] equation (12).

If one considers a system of more than three random walkers, one can apply the same considerations as above. The generalization of equation (11) for an arbitrary number of vertices N now reads:

$$p = \int_0^\infty \mathrm{d}t\, \gamma(1+t)^{-1-\gamma}(1-(1+t)^{1-\gamma})^{N-1} = \frac{(N-1)!(\gamma-1)^{N-1}}{(2\gamma-1)(3\gamma-2)\ldots(N\gamma-N+1)}. \tag{14}$$

To prove the last relation one changes the variable of integration in equation (14) to $z = t+1$ and performs the partial integration:

$$p = \int_1^\infty \mathrm{d}z\, \gamma z^{-1-\gamma}(1-z^{1-\gamma})^{N-1} = \frac{\gamma}{N(\gamma-1)}\int_1^\infty \frac{\mathrm{d}z}{z}\frac{\mathrm{d}}{\mathrm{d}z}(1-z^{1-\gamma})^N$$
$$= \frac{\gamma}{N(\gamma-1)}\int_1^\infty \frac{\mathrm{d}z}{z^2}(1-z^{1-\gamma})^N. \tag{15}$$

The change of variable $y = z^{1-\gamma}$ reduces the last integral to the standard form of the beta function:

$$p = \frac{\gamma}{N(\gamma-1)^2}\int_0^1 y^{(\gamma-2)/(1-\gamma)}(1-y)^N\,\mathrm{d}y = \frac{\gamma}{N(\gamma-1)^2}B\left(N+1, \frac{1}{\gamma-1}\right) \tag{16}$$

see equation (1.191.3) of [15]. Representing the beta function in terms of Γ-functions, $B(\mu, \nu) = \frac{\Gamma(\mu)\Gamma(\nu)}{\Gamma(\mu+\nu)}$ (equation (8.384) of [15]), one obtains then

$$p = \frac{(N-1)!\gamma}{(\gamma-1)^2}\Gamma\left(\frac{1}{\gamma-1}\right)\Big/\Gamma\left(N+1+\frac{1}{\gamma-1}\right) \tag{17}$$

which reduces to equation (14) by using the recurrence formula $\Gamma(x+1) = x\Gamma(x)$ repeatedly.

As an extension of our considerations for the case of the triangle, we obtain for N vertices that the mean number of steps and that of returns are related by $\langle n_r(t)\rangle \leqslant \langle n_s(t)\rangle \leqslant (N-1)\langle n_r(t)\rangle$. Therefore one can again surmise that the long-time diffusion coefficient D of a system of N random walkers connected by bonds goes as $(\gamma-1)^{-N}$ for $\gamma \to 1$. These considerations show that pinning effects are of much importance for large systems of coupled random walkers, such as polymer chains.

5. Conclusions

In this article we have analysed the motion of a rigid triangle; i.e. of a system of three random walkers coupled through holonomic constraints; the vertices jump according to

CTRWs with either exponential or algebraic WTDs. For exponential WTDs the system shows a simple diffusive behaviour. For algebraic WTDs the behaviour is much more complex due to the coupling between the temporal and the spatial aspects. In this case one observes two diffusive regimes (at short and long times) with a broad crossover region in between. The long-time diffusion coefficient is much smaller than the short-time one. The reason for the slow overall motion at long times is pinning: there is no overall translation of the triangle unless all three vertices move. We have shown that a simple approximation which takes into account pinning is in very good agreement with the numerical simulations for D and captures the most important statistical features of the system's behaviour. The generalization of our approach to the case of more than three vertices shows that the importance of pinning increases with the number of particles involved.

Acknowledgments

Thanks are due to Professor J Klafter for useful discussions. We acknowledge financial support through the DFG (SFB 60), through the Fonds der Chemischen Industrie and through a PROCOPE grant administrated by the DAAD.

References

[1] Orwoll R A and Stockmeyer W H 1969 *Adv. Chem. Phys.* **15** 305
[2] Verdier P H 1970 *J. Chem. Phys.* **52** 5512
[3] Alemany P A, Vogel R, Sokolov I M and Blumen A 1994 *J. Phys. A: Math. Gen.* **27** 7733
[4] Glarum S 1960 *J. Chem. Phys.* **33** 639
[5] Scher H and Montroll E W 1975 *Phys. Rev.* B **12** 2455
[6] Bendler J T and Shlesinger M F 1985 *The Wonderful World of Stochastics* ed M F Shlesinger and G H Weiss (Amsterdam: North-Holland) p 31
[7] Blumen A, Klafter J, White B S and Zumofen G 1984 *Phys. Rev. Lett.* **53** 1301
[8] Klafter J, Blumen A and Shlesinger M F 1987 *Phys. Rev.* A **35** 3081
[9] Blumen A, Klafter J and Zumofen G 1986 *Optical Spectroscopy of Glasses* ed I Zschokke (Dordrecht: Reidel) p 199
[10] Shlesinger M F 1988 *Ann. Rev. Phys. Chem.* **39** 269
[11] Eisenberg E, Havlin S and Weiss G H 1994 *Phys. Rev. Lett.* **72** 2827
[12] Schieber J D, Biller P and Petruccione F 1991 *J. Chem. Phys.* **94** 1592
[13] Cox D R 1967 *Renewal Theory* (London: Methuen)
[14] Prato D P and Pury P 1989 *Physica* A **157** 1261
[15] Gradstein I S and Ryzhik I M 1965 *Tables of Integrals, Series and Products* (New York: Academic)